Available online at www.sciencedirect.com

ScienceDirect

Procedia Engineering 14 (2011) 572–581

Procedia Engineering

www.elsevier.com/locate/procedia

The Twelfth East Asia-Pacific Conference on Structural Engineering and Construction

Experimental study of load-carrying cruciform joints Containing Incomplete Penetration and Strength Under-matching in Low and High Cycle Fatigue Regions

K. SAIPRASERTKIT[a*], T. HANJI[b†], and C. MIKI[c]

[a] *Department of Civil Engineering, Tokyo Institute of Technology, Japan*
[b] *Center for Urban Earthquake Engineering, Tokyo Institute of Technology, Japan*
[c] *Department of Civil Engineering, Tokyo Institute of Technology, Japan*

Abstract

Fatigue behaviors of load-carrying cruciform joints containing incomplete penetration and strength under-matching between base metal and weld deposit were studied. Low and high cycle fatigue tests were performed on specimens with five matching conditions and two sizes of incomplete penetration. Observation of the specimens revealed that crack propagation paths differ by low and high cycle loading conditions and that failure life was dominated by crack propagation. Besides, it was found that the effect of the strength under matching on the fatigue strength becomes large in low cycle fatigue region by significantly reducing fatigue life of the specimen. Moreover, local strain obtained from analysis model can be governing parameter to fatigue life of specimens.

Keywords: load-carrying cruciform joints, incomplete penetration, strength mismatching, low and high cycle fatigue strength

1. INTRODUCTION

Steel bridge bents have become an essential part and widely used in elevated highways. The connections between beams and columns in the steel bridge bents are designed to be full penetration welds. However, detailed investigation (Miki and Hirabayashi 2007) has revealed that incomplete penetration has existed in the connections of almost all steel bents. This means that the existing

* Presenter: Email: saiprasertkit.k.aa@m.titech.ac.jp
† Corresponding author: Email: hanji@cv.titech.ac.jp

1877–7058 © 2011 Published by Elsevier Ltd. Open access under CC BY-NC-ND license.
doi:10.1016/j.proeng.2011.07.072

beam-to-column connections can be identified as load-carrying cruciform joints with incomplete penetration as shown in **Fig.1**.

Two types of limit states can be supposed at the connections. One is the fatigue limit state due to traffic loads. Another is the ultimate limit state due to cyclic plastic deformation by seismic loads which trigger "low cycle fatigue damage". Thus, fatigue strength of the load-carrying cruciform joints with incomplete penetration should be investigated from low to high cycle fatigue regions.

The application of high strength steel can cause strength mismatch between base metal and weld deposit, particularly under-match, in which yield strength of the weld deposit is lower than that of the base metal. The effect of strength mismatch will become an important issue when high intensity stress such as earthquake is subjected to welded joints. Because behavior of the joints will be different by the strength mismatch since plastic deformation dominates in lower strength material.

In this study, the fatigue strength of the load-carrying cruciform joints containing the incomplete penetration and the strength mismatch was investigated in the low and the high cycle fatigue region.

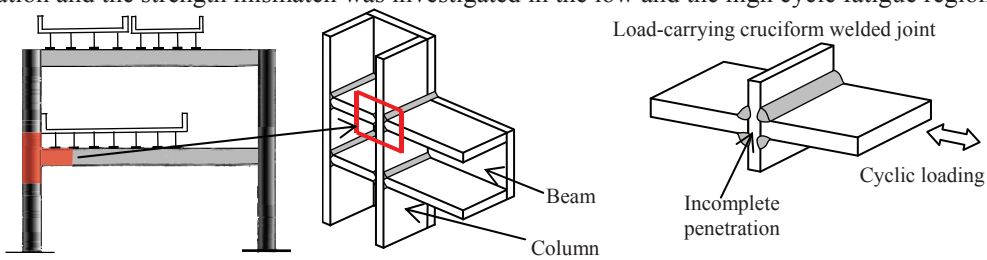

Fig.1 Load-carrying cruciform joint containing incomplete penetration.

2. TEST SPECIMENS

2.1. Fabrication methods

The configurations and dimensions of specimens are shown in **Fig.2**. Specimens were made of JIS SM490 and JIS SBHS500 class steel with the plate thickness of 28mm and 24mm respectively. Several welding condition, called O45, O25, U10 and U20 in this study, were applied to specimens in order to obtain different strength matching. For SM490, there are two types of specimens, named FL and PJP. The specimen type FL was fabricated by fillet welds while partial joint penetration groove welds was applied to specimen type PJP. Penetration ratio of FL and PJP type, which is the ratio between the length of unfused portion and thickness of the loading plate, were designed to be 100% and 60%. For SBHS500, there is only FL type. Weld root gaps were set to be almost 0mm.

2.2. Mechanical properties of weld deposit

2.2.1. Monotonic tensile loading tests on round bar specimen

In order to figure out the yield strength of material, monotonic tensile tests were carried out using round bar type specimens cut off from the weld deposit and the base metal of the specimen as shown in **Fig.3**. The tensile test results are also indicated in the figure.

Table 1 gives yield strength of the weld deposit and the base metal from the tensile tests. Matching ratio (WD/BM) implies that specimens with the value less than 1.0 is under matching joints and more than 1.0 is over matching joints. Thus, the specimen consists of approximately 25% and 45% over matching joints for SM490, 10% and 20% under matching joint for SBHS500, respectively. Specimens were named as shown in **Table 1** according to the welding type and condition.

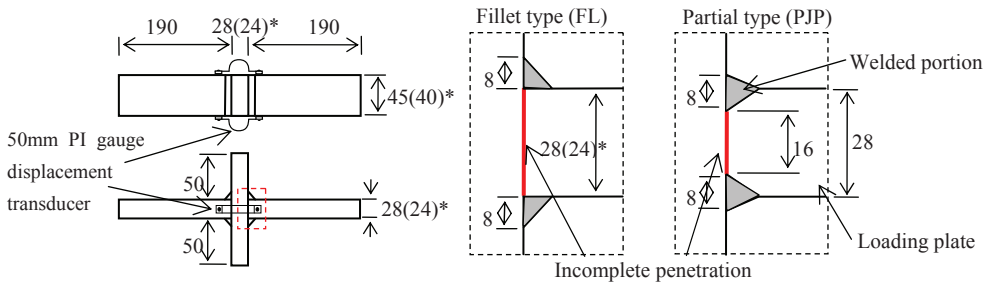

Fig.2 Specimens in mm.(*: number in a bracket shows dimension of specimen for SBHS500)

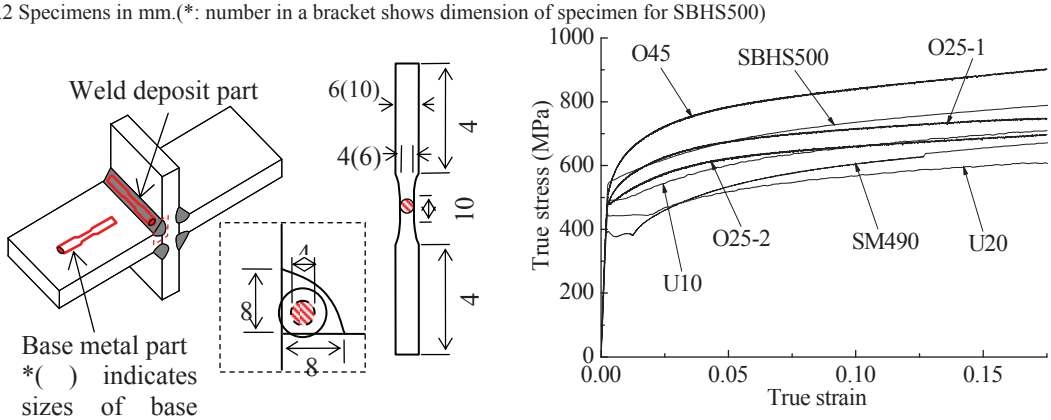

Fig.3 Round bar type specimen in mm and tensile test results of materials.

Table 1 Mechanical properties of materials.

Material		Cruciform joints		Specimen name	
		Yield strength (MPa)	Matching Ratio (WD/BM)	Fillet weld (FL)	Partial penetration weld (PJP)
SM490 (BM)		392	-		
Weld deposit (WD)	O45	565	1.44	FL-O45	PJP-O45
	O25-1	498	1.27	FL-O25-1	PJP-O25-1
	O25-2	494	1.26	FL-O25-2	PJP-O25-2
SBHS500 (BM)		554	-		
Weld deposit (WD)	U10	491	0.89	FL-U10	-
	U20	451	0.81	FL-U20	-

2.2.2. Incremental cyclic loading tests on round bar specimen

In order to obtained cyclic stress-strain behavior of base metal and weld deposit, incremental cyclic test was performed as shown in **Fig.4** using round bar specimen. The tensile test results are also indicated. Skelton curves from the incremental test locate higher than the tensile curves. Therefore, all material represents cyclic hardening behavior in most of the plastic strain region.

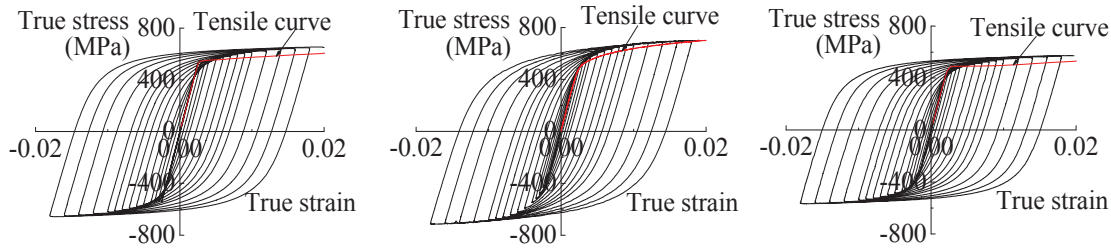

(a) Base metal, SBHS500 (b) Weld deposit, O45 (c) Weld deposit, U10

Fig.4 Incremental cyclic test result of base metal and weld deposit.

3. EXPERIMENTAL PROCEDURES

Monotonic loading test was conducted in addition to fatigue tests. The deformation around the weld portion was measured from 50mm displacement transducer attached to both side of loading plate over the weld root as shown in **Fig.2**. For low cycle fatigue tests, the tests were controlled by the value of the 50mm displacement transducer, giving the constant displacement range of 0.18, 0.23, 0.28 and 0.33mm. As displacement range 0.23mm, the test was stopped after 30% load drop in order to examine the crack length, while the others were continued until one weld bead failed. Small displacement rate approximately 0.0017-0.0082mm/sec was applied to the specimen. High cycle fatigue tests were conducted under load controlling condition. The stress range was calculated by dividing the load range with the measured weld throat area, which around 140 to 180MPa. The stress ratio was about 0.05. The loading rate was 10Hz. Two-strep block loading tests (beach mark test) were also performed. The test was continued until the specimen ruptured.

4. EXPERIMENTAL RESULTS

4.1. Characteristics of crack initiation and propagation

Fig.5 shows the observation of fatigue crack propagation at side surface of the specimen during the low cycle fatigue test. After the first cycle, large plastic deformation can be observed around the root tip, and a crack can be first detected at the side surface at 10 cycles then gradually propagated through weld deposit with the loading repetition. The results of beach mark tests are shown in **Fig.6**. From difference between load block applied to specimens and number of beach marks on fracture surface, the crack initiation life can be identified. It is noticed that the ratio of crack initiation life to fatigue life is almost zero, Ni/Nf=0.077 for FL-O45 and Ni/Nf=0.063 for FL-U10, in high cycle fatigue region. Previous research (Miki et al. 1981) has shown that the relation between crack initiation life and fatigue life can be governed by stress concentration at the crack initiation point, which means the ratio of crack initiation

point to fatigue life become small with increasing stress concentration factor. In load carrying cruciform joints, very high stress concentration factor occurs at weld root, thus, crack initiation can be consider to be extremely small in low cycle fatigue test.

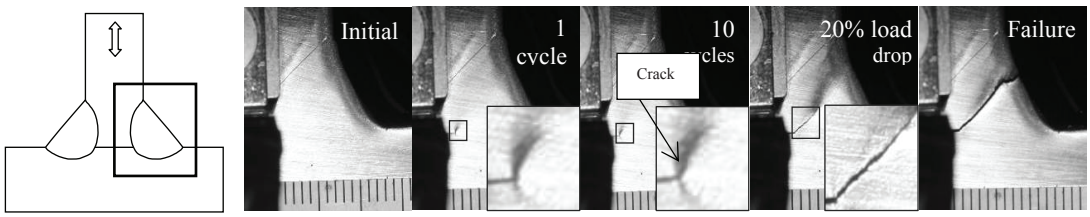

Fig.5 Crack propagation at side of low cycle fatigue test. (Specimen PJP-O45, 0.33mm disp.)

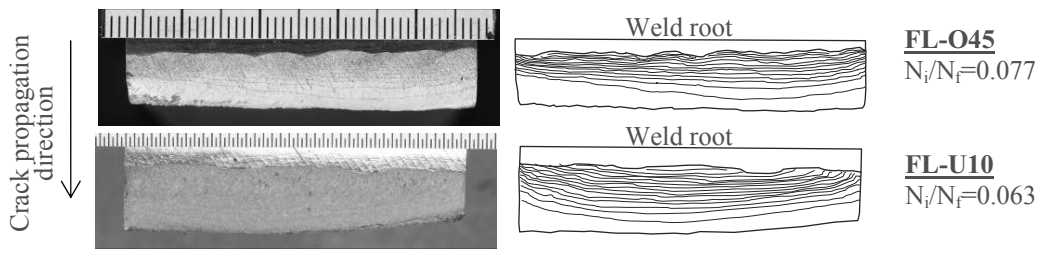

Fig.6 Beach marks of high cycle fatigue test.

4.2. Load-displacement hysteresis loops

Fig.7 shows an example of the load-displacement relationship in low cycle fatigue test. The maximum load is decreasing during load repetition, although the weld deposit of the specimen shows cyclic hardening behavior as illustrated in **Fig.4**. As mentioned above, this is because the crack was initiated at the early cycles and crack propagation is dominant in the total life.

4.3. Definition of fatigue life

Fig.8 shows the relation between ratio of maximum load of each cycle to maximum load at first cycle and number of cycles for low cycle fatigue test. The maximum load of specimen gradually decreased until the maximum load dropped by around 20% and suddenly declined after 30%. Thus, in this research, the low cycle fatigue life was defined as the number of cycle to 20% load drop.

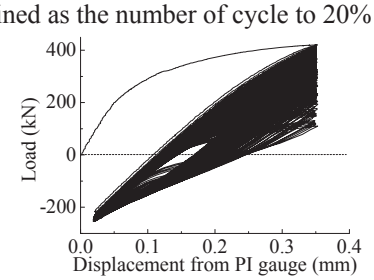

Fig.7 Load-displacement relation in low cycle fatigue test.(specimen FL-O45)

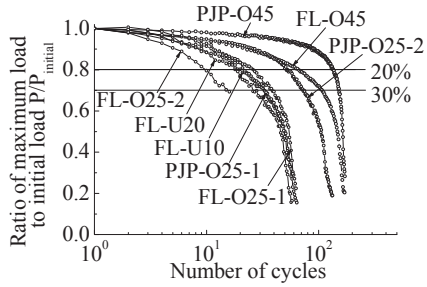

Fig.8 Relation between maximum load at each cycle and number of cycles

4.4. Crack propagation path

Fig.9 shows comparison of side surfaces of ruptured specimen for different loading condition, where illustrations display the location of weld deposit in dark gray. The crack propagation path of the tensile and the low cycle fatigue specimen are similar, which crack tends to propagate straight with low angle to a loading plate. While, the crack runs perpendicular to the loading direction then begins to propagate obliquely in the high cycle fatigue test.

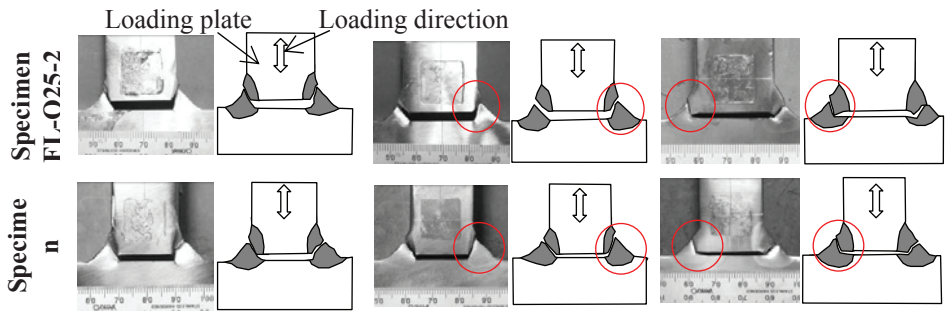

(a) Tensile test specimens (b) Low cycle fatigue test (c) High cycle fatigue test

Fig.9 Crack propagation paths. (Circles indicated failure from fatigue cracking)

4.5. Fatigue life

4.5.1. Low cycle fatigue tests

Fig.10 shows the relation between fatigue life and stress range for SM490 and SBHS500, respectively. The stress range was calculated by dividing the load range at the first cycle with the measured weld throat. It can be found that the strength matching has significant influence on the low cycle fatigue strength, as the specimen with lower matching ratio shows obviously lower fatigue strength. No noticeable difference between FL and PJP type specimens can be observed in **Fig.10(a)**. This may be because ratio of a/W (W = H1+tp/2) (Frank and Fisher 1979; Miki et al. 1993), where 2a is welded root size, tp is plate thickness and H1 is weld leg, which is one of the parameters to calculate stress intensity factor for the load-carrying cruciform joint, is relatively close in all specimens. Therefore, it is noticed that the parameter of a/W may be a factor governing the low cycle fatigue strength of the load-carrying cruciform joint.

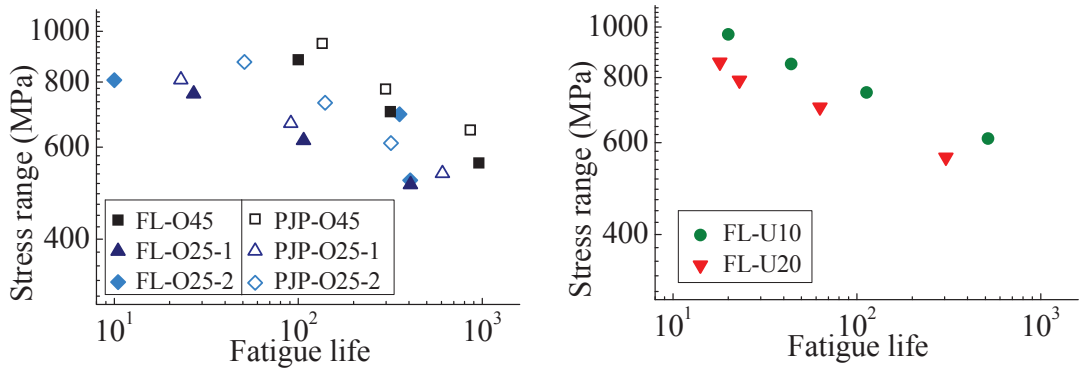

(a) SM490 specimen

(b) SBHS500 specimen

Fig.10 Results of low cycle fatigue tests. tests.

4.5.2. High cycle fatigue tests

Fig.11 shows the high cycle fatigue test result which is the relationship between the stress range and the fatigue life. The stress range is calculated by dividing the load range with the measured weld throat. S-N curve recommended in JSSC specification (Japanese Society of Steel Construction 1993) are also indicated. The results show that the fatigue strength for both the over and the under matching joint are almost same. Therefore, it is obvious that the effect of the strength mismatch is negligible in high cycle fatigue region.

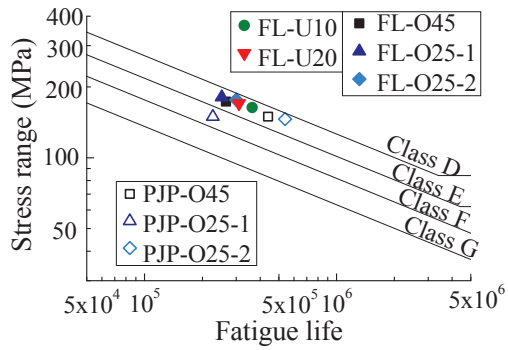

Fig.11 Results of high cycle fatigue tests.

5. Strain analysis

5.1. Analysis models

Elasto-plastic finite element analyses were performed to investigate strain field around root tip. Two dimensional analysis models under plane strain condition were used. One quarter symmetry model were created as shown in **Fig.12**. The shape and size of welded part was followed from the measurement of testing specimens. In order to avoid stress singularity at a root tip, a fictitious notch was adopted at the tip. The relatively small notch radius with 0.5mm was selected as it has little effect on load-displacement relationship between the analyses and the experiments. The boundary conditions were set to be the same as the experiments.

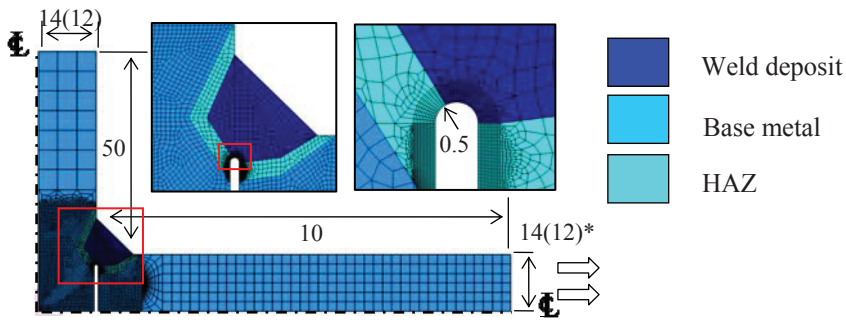

Fig.12 Analysis model in mm.(*: numbers in brackets show SBHS500 series)

5.2. Stress-strain relationships

A yield function given in eq.(1a) were employed for each material, consisting of isotropic hardening rule (eq.(1b)) and kinematic hardening rule (eq.(1c)).

$$f = \sigma - X - R - \sigma_y \tag{1a}$$

$$R = R_\infty \left(1 - \exp\left(-b \cdot \varepsilon_p\right)\right) \tag{1b}$$

$$X = X_{\infty}\left(1-\exp\left(-\gamma\cdot\varepsilon_{p}\right)\right) \tag{1c}$$

where, R is the isotropic hardening, X is the back stress, R∞, b, X∞, γ are material parameters and εp is plastic strain. The isotropic and kinematic parameters were identified based on material tests shown in **Fig.13**. In the test, round bar specimen in **Fig.3** were used. **Fig.13** also gives the material parameters in isotropic and kinematic hardening. In all models, the same hardening parameters as weld deposit were assigned to HAZ, but HAZ was assumed to have 20% higher yield stress than that of weld deposit.

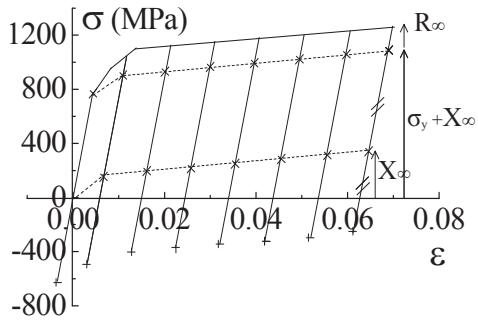

Material		σy (MPa)	Isotropic hardening		Kinematic hardening	
			R∞ (MPa)	b	X∞ (MPa)	γ
SM490 (BM)		304	143	4	233	33
Weld deposit (WD)	O45	435	387	1	292	106
	O25-1	367	95	3	284	163
	O25-2	351	223	1	283	124
SBHS500 (BM)		493	143	2	201	97
Weld deposit (WD)	U10	446	96	1	212	96
	U20	362	98	1	180	69

Fig.13 Material parameters.

5.3. Local strain approach

Fig.14 shows relation between local strain range at the weld root and fatigue life. The local strain range was obtained in elements along the fictitious notch which has maximum value of equivalent plastic strain range. It is noticed that local strain can be used to arrange the fatigue strength of specimens in both low and high cycle fatigue region.

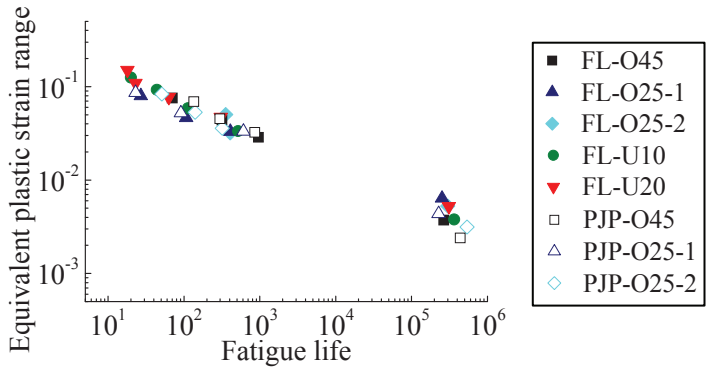

Fig.14 Relation between equivalent plastic strain range and fatigue life.

6. CONCLUSIONS

1. Crack initiation life is very small, thus crack propagation is dominant in the total life.
2. Crack propagation path of low and high cycle fatigue are different.
3. Strength matching between the weld deposit and the base metal has significant influence on the low cycle fatigue strength, however, it can be negligible in high cycle fatigue region.
4. Local strain obtained from elasto-plastic FEM with fictitious notch can be use to evaluate both low and high cycle fatigue strength of load carrying cruciform joints with a unique curve.

REFERENCES

[1] Frank KH and Fisher J.W (1979). Fatigue strength of fillet welded cruciform joints, J. Struct. Div., ASCE, Vol.105, No.ST9, pp.1727-1740.

[2] Ishii Y and Iida K (1969). Low and intermediate cycle fatigue strength of butt welds containing weld defects, J. JSNDI, Vol.18, No.10, pp.443-474.

[3] Japanese Society of Steel Construction (1993). Fatigue design recommendations for steel structures, Gihodo Shuppan. (in Japanese)

[4] Miki C and Hirabayashi Y (2007). Fatigue damage cases due to inappropriate fabrication in steel bridge structures, Doboku Gakkai Ronbunshuu A, JSCE, Vol.63, No.3, pp.518-532. (in Japanese)

[5] Miki C, Tateishi K, Fan H and Tanaka M. (1993). Fatigue strengths of fillet-welded joints containing root discontinuities, Int. J. Fatigue, Vol.15, No.2, pp.133-140.

[6] Miki C, Nishimura T, Tanabe H and Nishikawa K (1981). Study on estimation of fatigue strengths of notched steel members, Proc. JSCE, No.316, pp.153-168